

SIMULATION OF MICROFLUIDIC MIXING USING ARTIFICIAL CILIA

M.G.H.M. Baltussen
Eindhoven University of Technology
m.g.h.m.baltussen@tue.nl

J.M.J. den Toonder****¹, F.M. Bos, P.D. Anderson*
*Eindhoven University of Technology
**Philips Research Laboratories
j.m.j.d.toonder@tue.nl, femke@beryllium.net, p.d.anderson@tue.nl

KEY WORDS

Micromixer, inertial flow, mixing analysis, computational fluid dynamics, optical coherence tomography

ABSTRACT

Our recently developed micro-mixer based on artificial cilia shows good mixing over relatively short length-scales [1], which was unexpected. In this paper we present a numerical tool and use it to simulate the micro-mixer to explain the observed effects. The tool consists of a fully coupled fluid-solid interaction model, which is solved with a finite element method, and a particle tracking scheme. The former computes the motion of fluid and solid for one actuation cycle of the cilia and the latter tracks the position of passive particles for several cycles using the calculated velocity field. Two parameter sets are computed, one including and one excluding fluid inertia. The obtained particle distributions after fifty cycles show that net fluid motion is in the direction of the recovery part of the cycle for the inertialess case and in the direction of the actuation part of the cycle for the inertial case. This implies that by controlling the cilium velocity, which controls the Reynolds number, the flow direction can be controlled for a given system. The simulated intermediate particle distributions agree very well with optical coherence tomography data for the inertial case, whereas the inertialess simulations show completely different behaviour. Therefore it is concluded that inertial effects play a crucial role in the efficient mixing in this micro-mixer, which was not expected since the dimensions are in the sub-millimetre range.

1. INTRODUCTION

The analysis of bio fluids (blood, saliva, urine) is a widely used clinical assessment technique. By combining all analysis steps into one device and decreasing the dimensions of this device, the amount of required biofluid is reduced and the analysis time is shortened. A common step during the analysis is a chemical reaction between the biofluid and an additional functional chemical. In order to obtain high reaction rates, the interface between the reactants has to be large, since diffusion is still too slow, even at the small length-scales (sub mm) of this device. Since the flow is also far from turbulent, special mixing techniques have to be developed, to obtain chaotic mixing and hence rapid increase of interfacial area. This can either be done by adapting the geometry of the channel, which is called a passive mixer, or by actively controlling the fluid, which is called an active mixer. Examples of both can be found in Nguyen *et al.* [2]. Most of the active mixers in this review are based on pressure, electro kinetic or acoustic disturbances. Recently however we have developed an active micromixer

¹ Corresponding author

which is based on electrostatically operated polymer micro-actuators, or artificial cilia [1]. Cilia are the hairs on the outside of micro-organisms which they use to propel themselves. Since these organisms can reach quite high speeds compared to their length, it seems a promising fluid manipulation actuator at micro-scales. Since the fluid velocities are low and the cilium dimensions are small, the flow is inertialess and net fluid flow can only be obtained by asymmetric motion of the cilium. Therefore a semi-circular micro-actuator was designed, and several rows of these cilia were placed in a channel, see Figure 1. By applying a voltage difference between the cilia and an electrode on the surface, an electrostatic attraction force is induced and the curled micro-actuator rolls out and extends over the surface. After switching off the voltage, the structure rolls back to its original curled shape by elastic recovery. The cilia were organized in segments of 1x1 mm, and the mixing of two fluids in a Y-shaped channel was studied for the different configurations of cilia in segments. It was found that efficient mixing took place within 2 element lengths and within 1 second, which was not expected since the fluid motion was assumed to be inertialess, thus requiring longer mixing lengths.

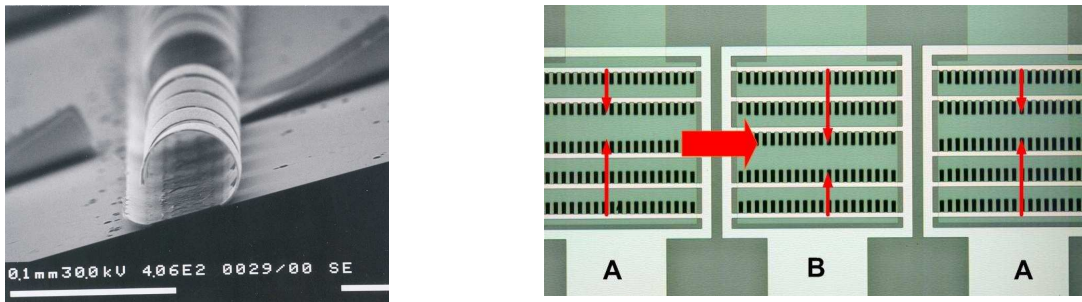


Figure 1: Left: Electronmicrograph of the developed artificial cilia, with a length of about 100 μm and a thickness of 1 μm . Right: top view of the channel, showing three segments or unit cells of 1x1 mm containing five rows of cilia. The main flow is in the direction of the large arrow. The smaller arrows point in the direction of the unrolling direction of the cilia. The unit cells are placed in an alternating pattern in the main channel.

In this paper we present a numerical model that can predict the fluid and cilium motion in two dimensions and the reason for the observed exceptionally fast mixing will be shown.

2. OPTICAL COHERENCE TOMOGRAPHY

The effect of the artificial cilia on the fluid in a channel was studied by optical coherence tomography (OCT), which enables flow visualisation of a cross-section of the channel. OCT is an imaging technique based on the principle of low (temporal) coherence interferometry [3]. By taking a cross-section, perpendicular to the main flow direction, the transverse flow is measured. The transverse flow causes the mixing. Since optical access to the channel in the main flow direction is limited, confocal microscopy and micro PIV could not be used for flow visualization and OCT had to be used, since it places less stringent requirements on the optical access.

2.1 Materials

In this case an OCT setup has been used from Thorlabs (Spectral Radar OCT Imaging System with OCT microscope), which has an axial resolution of 4.7 μm in water, a lateral resolution of 9.2 μm and can capture images at 5.6 frames/s. We used a Y-shaped channel with a width of 1 mm and a height of 0.5 mm, made from PDMS, attached to a glass substrate on which the cilia were processed in the desired configurations.

The exact structure and materials for the cilia, as well as the processing techniques used for making them can be found in [1].

Experiments were conducted in silicone oil with a viscosity of 9.3 mPas, which was either clear or saturated with TiO_2 particles in order to obtain as much optical scattering contrast in the oil as possible, resulting in clear OCT images.

2.2 Methods

Both the Y-shaped entrance channels were connected to syringe pumps pumping at $6\mu\text{l}/\text{min}$, which corresponds to a mean velocity of 0.2 mm/s . One entrance channel was fed with transparent oil and the other with oil with particles. As soon as two distinct flows were observed, a recording was started, without actuating the cilia. Shortly after the recording was started, the MEMS were actuated at a frequency of 80 Hz and a voltage of 90 Volts . The evolution of the flow pattern over time was then recorded at a single cross-section of the channel.

3. MODELLING

A 2D cross-section of the channel in Figure 1 was modelled. The configuration studied, corresponds to that of Figure 1, with three cilia pointing left and two right, as is shown in Figure 2.

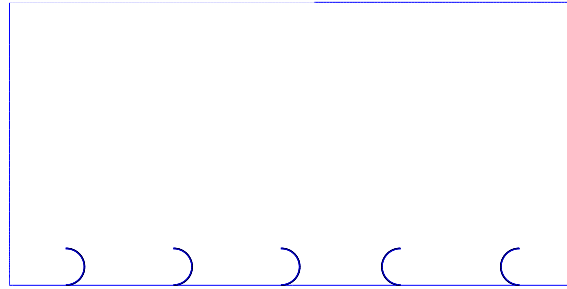


Figure 2: The cross-section of the micromixer based on artificial cilia. The width W of the channel is 1 mm , the height H is 0.5 mm , the length of the cilia L is $100\ \mu\text{m}$ and their thickness t is $1\ \mu\text{m}$.

The fluid and solid domain surrounding and comprising a single cilium are sketched in Figure 3.

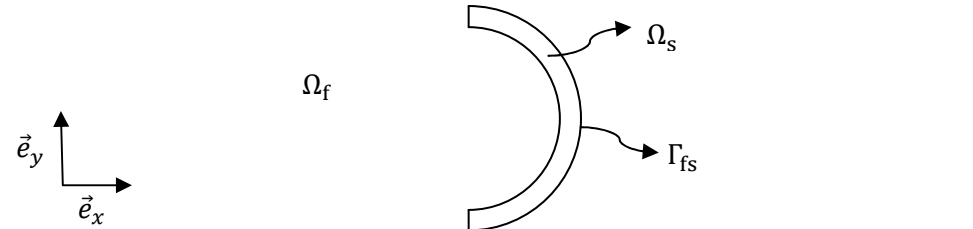


Figure 3: The fluid and solid domain near a single cilium.

Both the fluid and the solid were modelled as a continuum and both are taken incompressible. In addition to that the solid was taken to be inertialess. By scaling the time, displacement, velocity and spatial gradient with the unrolling time of the cilia t_{roll} , the length of the cilia L , L/t_{roll} , and L respectively the following non-dimensional forms of the mass and momentum equation for fluid and solid are found:

$$\begin{aligned} \text{Re} \left(\frac{\partial \vec{u}}{\partial t} + \vec{u} \cdot \nabla \vec{u} \right) &= \nabla \cdot 2\mathbf{D} - \nabla p \\ \nabla \cdot \vec{u} &= 0 \\ -\text{El} \nabla \cdot (\mathbf{B} - \mathbf{I}) + \nabla p &= \vec{f}_{\text{app}} \\ J - 1 &= 0 \end{aligned} \quad (1)$$

where \vec{u} is the fluid velocity, \mathbf{D} is the rate of deformation tensor, p is the pressure, in both the fluid as solid $\mathbf{B} = \mathbf{F} \cdot \mathbf{F}^T$ is the Finger tensor containing the deformation gradient tensor \mathbf{F} , \vec{f}_{app} the applied force and $J = \det \mathbf{F}$ is the third invariant of \mathbf{F} . In addition the following dimensionless groups are found:

- $\text{Re} = \frac{\rho L^2}{\eta t_{\text{roll}}}$, the Reynolds number which is the ratio between inertial forces and viscous forces in the fluid (ρ is the density of the fluid and η the viscosity),

- $El = \frac{G}{f_0 L}$, the elasticity number, which is the ratio between elastic and applied forces (G is the elastic modulus of the cilium, and f_0 the maximum applied electrostatic force).

The electrostatic actuation force is modelled as a volume averaged surface force, based on the forces on the conductor in a parallel plate capacitor [4], given by the following equation:

$$\vec{f}_{\text{app}} = \frac{1}{t} (\vec{n} \cdot \sigma_M) = -\frac{1}{t} \frac{\varepsilon}{8\pi} \frac{\Delta V^2}{h^2} \vec{e}_y, \quad (2)$$

where $\vec{n} = -\vec{e}_y$, the normal direction with respect to the upper conductor, $\sigma_M = \frac{\varepsilon}{4\pi} \left(\vec{E}\vec{E} - \frac{\vec{E} \cdot \vec{E}}{2} \mathbf{I} \right)$, the Maxwell stress tensor in a dielectric medium, containing the electric field $\vec{E} = -\frac{\Delta V}{h}$, with ΔV the electrical potential difference applied between the upper electrode and the ground electrode, h the vertical distance between both electrodes, and ε the dielectric constant of the fluid in between the two conductors. By computing the force on the upper electrode from the Maxwell stress tensor, a surface force is obtained which is averaged over the thickness of the cilium resulting in a body force. This force is switched on until the cilium is completely rolled out, after this event it is switched off and the cilium recovers elastically.

The solid and the fluid motion are coupled on the solid boundary via the following kinematic relation:

$$\vec{\dot{d}} - \vec{u} = \vec{0} \quad (3)$$

where $\vec{\dot{d}}$ is the time derivative of the displacement. Since this constraint is applied to the system with a Lagrangian multiplier, the force balance at the interface is also attained.

3.1 Methods

In order to compare simulations of the model with OCT experiments, distributions of trace particles suspended in the fluid have to be calculated at regular intervals. Since the particle distributions are measured during several seconds, and the cilia are actuated at 80 Hz, many cycles have been performed in the experiments. Since the computation of one cycle takes about 6 hours, a complete simulation of several seconds of actuation would take too long. It is however not necessary to perform this time consuming simulation, since the solution will become periodic after several cycles. Therefore one complete cycle was simulated with a direct numerical simulation (DNS) and the obtained velocity field was used to perform particle tracking simulations for 50 cycles. Initially a rectangular block of particles was placed in the right half of the domain.

4. NUMERICAL IMPLEMENTATION

The set of equations (1) is solved with a finite element method. Euler backward time integration scheme is used, which allows for variable time steps and the non-linear set of equations is linearised using Picard iteration for the solid momentum equation and Newton iteration for the fluid momentum equation. The kinematic constraint (3) is applied via collocation points in a fictitious domain framework [5]. For the solution of this coupled non-linear problem it is best to obtain solutions for the fluid and solid problem at the same state. Solving the resulting set of equations in a fully coupled manner ensures this, hence this approach will be used.

The cilia roll out onto the lower channel wall; hence this contact has to be modelled in order to prevent the crossing of cilia with the wall. During iteration nodal points on the boundary of the cilium can cross this wall however, as depicted in Figure 4.

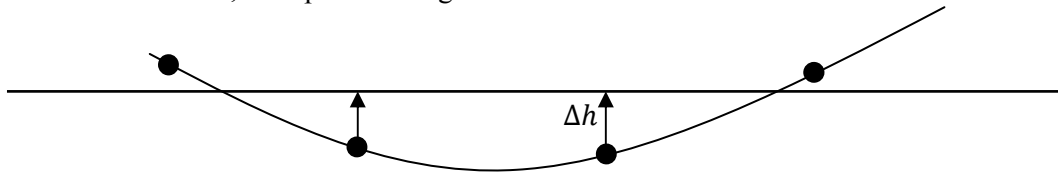


Figure 4: Cilium nodes (●) crossing the lower channel wall. Each node is displaced upward by Δh , the vertical distance to the wall.

These nodal points are placed back on the channel wall, and since no slip boundary conditions hold at the wall, the coupling condition (3) is released and the following relation for the solid displacement is given:

$$\vec{d} = \Delta h \vec{e}_y \quad (4)$$

This displacement automatically gives a force on the elastic cilium, which equals the reaction force of the wall onto the cilium. When the forcing term in the momentum equation is switched off, the stored elastic energy is strong enough to pull the cilium from the wall. At this time (4) is replaced by (3) again.

The fluid mesh contains 200 elements in the horizontal direction and 60 elements in the vertical direction. Each cilium consists of 40 elements in the axial directions and 4 in the thickness direction. Both the fluid and the solid elements are quadrilateral elements with quadratic interpolation of the velocity and the displacement and linear interpolation of the pressure.

5. RESULTS

Two simulations have been performed with the parameters listed in Table 1.

Parameter	Value
ρ	0-9300 kg/m ³
η	9.3 mPas
G	1 GPa
L	0.1 mm
t_{roll}	1 ms
f_0	512 GN/m ³

Table 1: Solid and fluid properties.

The corresponding Reynolds number and elasticity number are $Re=0, 10$ and $El=19.5$. The range of parameters implies that the effect of fluid inertia is investigated, since it does not play a role at $Re=0$ and it may play a role at $Re=10$. The motion of the cilia can be characterized by the path followed by the tip of the leftmost cilium of Figure 2. The tip is chosen, since it sweeps the largest area. The simulated path is given in Figure 5, and consists of an unrolling part (lower line, blue), and an elastic recovery part (upper line, red).

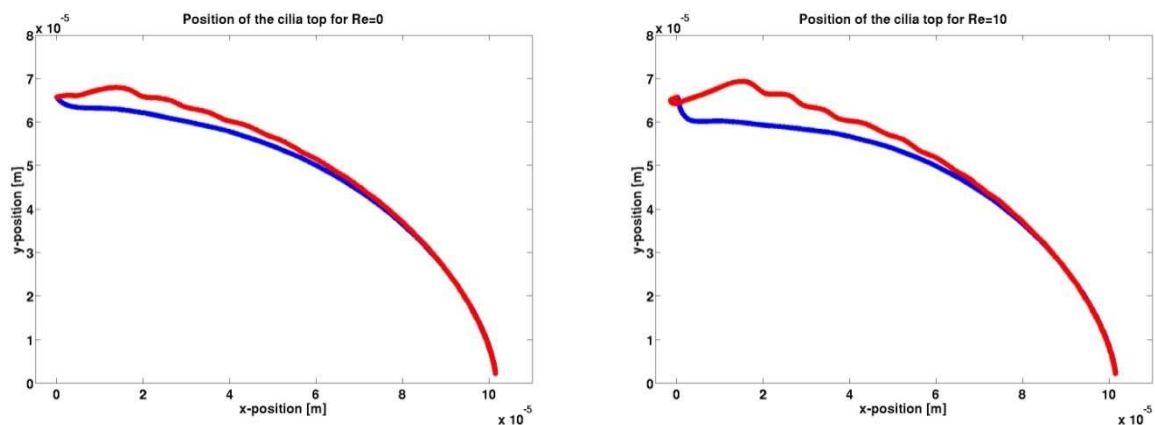


Figure 5: Simulated tip the position of the leftmost cilium of Figure 2, during a single cycle for $Re=0$ (left) and $Re=10$ (right). Unrolling motion is the lower part of the graph (blue), recovery or rolling the upper part (red).

From Figure 5 it can be seen that there is little asymmetry in the motion of the cilium for Reynolds numbers. For the Stokes flow ($Re=0$) this means that there will be not much net flow, since this is proportional to the swept area (i.e. the area enclosed by the unrolling and recovery curves), which is small for $Re=0$. For $Re=10$ this cannot be said from this figure alone, since the time scales of the

unrolling and rolling have to be known too and inertia may play a role too. Furthermore for $Re=0$ the net flow will be to the left, since the rolling path sweeps more area than the unrolling path.

If the particle distributions after 50 cycles for both Reynolds numbers are compared it is observed that the inertial flow direction is opposite to the inertialess case, see Figure 6. In practice the Reynolds number, defined in Equation 1, can be controlled by controlling the unrolling timescale. By changing the magnitude of the applied voltage, the unrolling time can be altered and by the change in Reynolds number the flow direction can be controlled.



Figure 6: Simulated particle distributions after 50 cycles for $Re=0$ (left) and $Re=50$ (right).

In Figure 7, the simulated particle distributions at different cycles are compared with the images obtained from OCT. As is expected from the previous paragraph, the Stokes flow does not agree at all with experimental data, whereas the simulation results and the experimental data show good agreement for the inertial case.

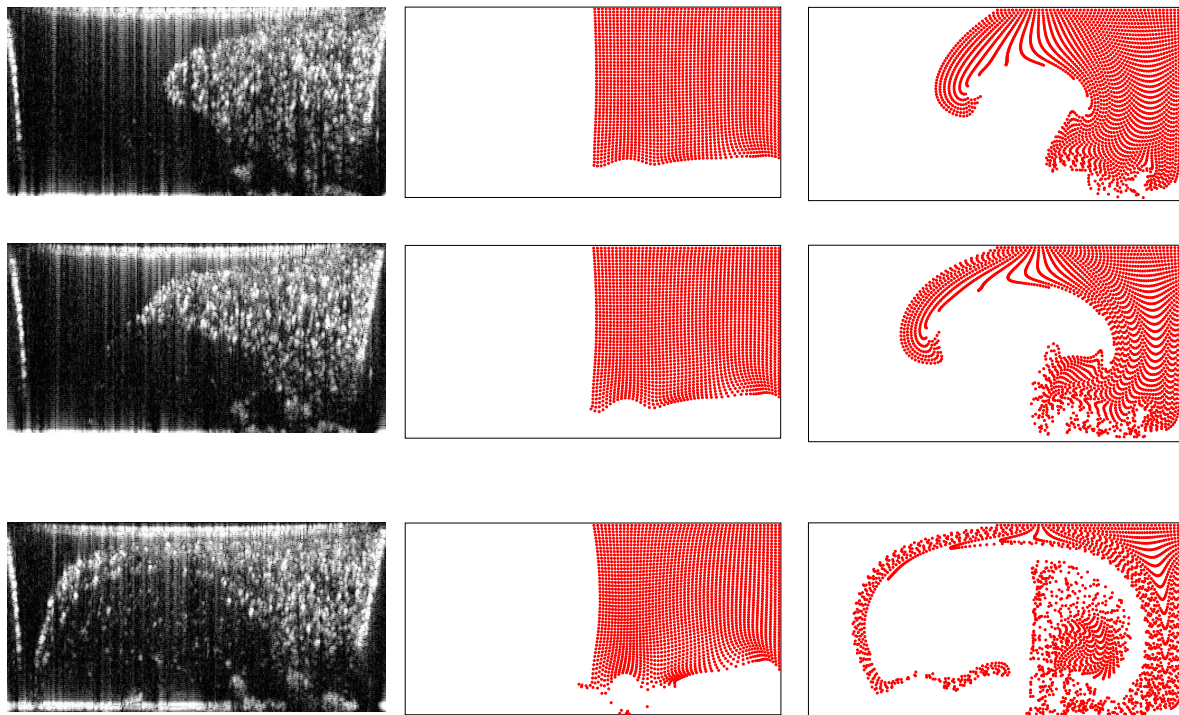


Figure 7: Left: images from OCT measurement. Middle: simulated tracer particle positions for $Re=0$ simulations. Right: simulated tracer particle positions for $Re=10$. The experimental data are shown at frame 15, 25, and 68, both simulations at cycle 6, 10 and 22 from top to bottom.

Note that the OCT images are given at frames which have an interval of $1/5.6$ s, whereas the simulated cycles take only 4ms. This is mainly explained by the fact that the actuation force in the simulations is shutdown immediately after the cilium is fully unrolled, which is after 1 m both in the simulations as well as the experiments [1]. In the experiment however the cilium remains attached to the wall until 6.25 ms, since the electrostatic force is not switched off immediately. The 6.25 ms corresponds to half the switching time at 80 Hz. Rolling back takes about 4 ms in both simulations as experiments. Therefore a complete cycle take about 5 ms in the simulations and 12.5 ms in experiments, during which the cilia move continuously in the simulations and stay “idle” in the experiments for some time.

In this idle time inertial effects continue and could lead to an increase or decrease of the net flow. Figure 7 suggest the latter case, since a comparison of the frame numbers indicates that the experimental mixing is less (effective). So mixing could be improved by increasing the actuation frequency. Another possibility is the fact that the Reynolds number in the experiments is less than 10, so inertia is less important and its effects are less visible. It is clear however that simulations containing inertial forces in the fluid are in much better agreement with the experiments than the Stokes simulations. We therefore conclude that inertia is of importance in the observed mixing process. Inertia leads to better distributive mixing for the micromixer based on artificial cilia, even at low Reynolds numbers.

6. CONCLUSION

We have investigated the role of fluid inertia in the micromixer based on artificial cilia. Optical coherence tomography (OCT) was used to analyse a cross-section of this mixer. We developed a numerical model used it for direct numerical simulation of the problem for $Re=0$ (Stokes flow) and $Re=10$ (inertial flow). The resulting velocity field was used to compute the position of passive particles in the fluid over time, which is equivalent to observing the TiO_2 tracer particles in the OCT experiments. The simulated tip position of the leftmost cilia showed only little asymmetry implying a very limited net flow in the Stokes case. The nature of this minor asymmetry causes a small net flow in the direction of the recovery stroke. For $Re=10$, however, the net flow is much higher and in the direction of the actuation or unrolling stroke. The inertial computations were in close agreement with the OCT measurements, whereas the inertialess simulations were no, and therefore we conclude that inertia is of importance in the observed mixing process, even though the dimensions of the channel and the cilia are in the sub-millimetre range. By changing the magnitude of the electrostatic actuation force, the unrolling velocity of the cilia can be controlled and hence the Reynolds number is controllable. This gives the possibility of actively controlling the flow direction.

ACKNOWLEDGEMENTS

This work is part of the European project 'Artic' (Framework 6, STRP 033274).

REFERENCES

- [1] Toonder, J.M.J. den, Bos, F.M., Broer, D.J., Filippini, L., Gillies, M., Goede, J. de, Mol, G.N., Talen, W., Wilderbeek, J.T.A., Khatavkar, V., & Anderson, P.D. (2008). Artificial cilia for active micro-fluidic mixing, *Lab Chip*, **8**, 533-541.
- [2] Nguyen, N.T., & Wu, Z.. (2005) Micromixers – a review, *J. Micromech-Microeng*, **15**, 1-16.
- [3] Bouma, B.E., Guillermo, J., & Tearney, G.J. (2002). *Handbook of Optical Coherence Tomography*. first edn. Dekker inc.
- [4] Landau, L.D., Lifshitz, E.M., & Pitaevskii, L.P. (1984). *Electrodynamics of Continuous Media*. second edn. Butterworth-Heinemann, page 29.
- [5] Khatavkar, V., Anderson, P.D., Toonder, J.M.J. den, & Meijer, H.E.H. (2007). Active micromixer based on artificial cilia. *Phys. Fluids*, **19**, 083605.